Activated carbon obtained from banana peels for the removal of As (III) from water

Jasana Maharjan[*], and Vinay Kumar Jha[**]

[*]Department of Chemistry, Padma Kanya Multiple Campus, Bagbazar, Kathmandu, Nepal.

[**]Central Department of Chemistry, Tribhuvan University, Kirtipur, Kathmandu, Nepal.

Abstract: Present study deals with the preparation of activated carbons from banana peels. The banana peels were subjected to pyrolysis at 700 °C for 1 hour in open air (O_2-BP), nitrogen gas (N_2-BP) and mixture of nitrogen gas and water steam generated to 60-70 °C (N_2+H_2O-BP). The raw and activated carbons from banana peels were characterized by XRD, FTIR and methylene blue adsorption methods. The N_2+H_2O-BP was used for the adsorption of As (III) ions from aqueous solution. Various parameters affecting the adsorption process like pH (4 to 10), contact time and initial metal ion concentration were varied during the adsorption process. The optimum pH for As (III) adsorption was at 7. An equilibrium time of 2 hours was required for adsorption of As (III) ion. The adsorption isotherms were determined by using Langmuir and Freundlich isotherms and the experimental data were better fitted to Langmuir equation with high coefficient of determination value (R^2 = 0.9934). The experimental data fitted well to pseudo second order kinetic model with rate constant value of 0.0111 g/ (mg·min). The adsorption of As (III) on banana peels was spontaneous and followed physiosorption mechanism. The value of separation parameters (R_L) was found to be $0 < R_L > 1$ for all initial As(III) ion concentrations showed good adsorption of As(III) into banana peels.

Keywords: Adsorbent; Adsorption isotherm; Banana peels; Kinetics.

Introduction

Water which is the most important resource for the existence of life in earth is being polluted day by day due to the urbanization, industrialization and rapid population growth. Industries like electroplating; battery manufacturing, textile, carpet, dyeing etc. are destroying the quality of water by dumping their wastes into the water sources[1]. Industrial waste consists of heavy metals like Pb, Zn, As, Cd, Co, Ni, Hg, etc. as their major constituents. Accumulation of these heavy metals above their permissible limit, seriously affect food chain, aquatic life and public health[2]. Arsenic is one of the toxic heavy metal derived from the Greek word 'arsenikon' which means yellow orpiment and was isolated in 1250 A.D. by Albertus Magnus. It is notorious king of all poison and has been classified by the World Health Organization as a group 1, human carcinogenic substance[3]. There are three allotropic forms of arsenic *i.e.* yellow, black and grey among which the most stable form of arsenic is silver grey brittle crystalline solid[4]. It is a metalloid known to be the 20th most abundant element in the earth. It is a constituent in approximately 245 mineral species, which are predominantly ores containing sulfide, copper, nickel, lead, cobalt, or other metals[5]. Arsenic exists with several oxidation states as -3, 0, +3 and, +5 in aqueous media[6]. It occurs in rock, soil, air and in natural water mainly as

trivalent arsenite As (III) and pentavalent arsenate As (V). Arsenic (III) is 60 times more toxic than As(V), as it is more cytotoxic, genotoxic, mobile, and soluble[7, 8]. Arsenic (V) is stable in oxidative condition and exists as a monovalent ($H_2AsO_4^-$) or divalent ($HAsO_4^{2-}$) anion, while AS(III) is stable in reductive conditions and exists as an uncharged (H_3AsO_3) or anionic species ($H_2AsO_3^-$). Arsenic(III) is hard acid and forms complexes with oxides and nitrogen and As (V) is soft acid and forms complexes with sulfides[9]. With the accumulation of trivalent intermediates in the human body, there is a higher possibility of developing arsenic-induced diseases[10,11]. Environmental forms of arsenic includes, arsenious acids (H_3AsO_3, $H_3AsO_3^-$, $H_3AsO_3^{--}$), arsenic acid (H_3AsO_4, $H_3AsO_4^-$, $H_3AsO_4^{--}$), arsenates, arsenate, methyl arsenic acid and dimethyl arsenic acid, arsine, etc. The level of arsenic in fish and sea food may be high due to adsorption of arsenic from water. But, fortunately, fish contains significant amount of organic forms of arsenic such as monomethyl arsenic acid (MMAA) and dimethyl arsenic acid (DMAA) which are harmless compared to inorganic forms of arsenic. Organic forms of arsenic are quantitatively in significant and are mostly found in surface water. The toxicity of different arsenic species varies in the order:

Arsenite > Arsenate > Monomethyl arsenate > Dimethyl arsenate

Presence of arsenic in water especially in ground water is global environmental health problem and is affecting large number of people. In 2012, it was estimated that about 202 million people worldwide are exposed to arsenic concentrations in drinking water above 50 μg/L[12]. The largest risk of arsenicosis is in Bangladesh, West Bengal, India, Argentina, China, Hungary, Mexico, Taiwan, USA, Japan including western Terai region of Nepal[13]. The primary source of exposure to arsenic is food, drinking water, soil and arsenic based pesticides. Arsenic may enter lakes, rivers, underground water by weathering of rocks, volcanic activities, burning of fossil fuels, incineration of arsenic containing compounds, arsenical pesticides, fertilizers, herbicides, pharmaceuticals etc[14].

Arsenic poisoning is heightening in Asia and arsenic in Terai is a new problem. In Nepal, 47% population lives in Terai region and 90% rely on ground water as major source of drinking water. The condition of arsenicosis is the worst in Nawalparasi and its neighboring districts like Bara, Parasa, Kapilvastu, Rautahat, Siraha etc[15]. In Nawalparasi district, 4000 wells contain arsenic level above 50 ppb. A study by Japan International Corporation Agency (JICA) and the Environment in Kathmandu valley showed that 72% of deep tube well failed to meet WHO standard of 10 ppb and 12% failed to meet Nepal standard of 50 ppb. High prevalence (18.6%) arsenicosisis is found in Patkhouli village in Nawalparasi where 95.8% tube well is contaminated with arsenic. In Nawalparasi district, 95.6% population has been found with symptoms of Melanosis and 57.8% population with keratosis on palms, trunk, feet and 3.3% population with leucomelanosis[16].

There are different methods for arsenic removal which are physio-chemical and biological methods. Owing to the toxicity of Arsenic contamination, various physio-chemical methods have been developed like coagulation, precipitation, membrane separation, ion exchange, reverse osmosis, etc[17]. But these methods have certain drawbacks like incomplete recovery, expensive and production of toxic sludge. Recently, cost effective and eco-friendly bio-adsorption has been gaining attention to researchers. Literature shows that agricultural wastes like rice husk, jute stick, rice polish, sugarcane bagasse etc. either in natural or modified form is highly effective for arsenic adsorption from wastewater. Among different methods for arsenic removal, adsorption is the most suitable simple efficient and economical method but due to the cost factor, bio-adsorption is gaining more attention. In this method, industrial and agro waste such as red mud, fly ash, zeolite, blast furnace slag, hydroxide and bio adsorbents are used for the adsorption of arsenic.

Banana is the most popular herbaceous plant of family *Musaceae* originated from tropical region of Southeast Asia, in the jungle of Malaysia. It grows up to height (2-8

m) with leaves of 3.5 m in length. It is grown in more than 150 countries producing 105 million tons of fruit per year. India, China, Uganda, Philippines, Ecuador, Brazil, Colombia, Cameron, Tanzania etc. are the major countries for producing banana in the world[18]. It is a high value agricultural product and major fruit in Nepal in terms of potential growing area, production and domestic consumption. It is grown in 68 district of Nepal with total productive areas of 11,864 hectares with total annual production, 182,005 tones[19]. Banana is protected by peel which is discarded after inner fleshly portion is eaten. It is outer envelope of banana fruit and byproduct of banana consumption and processing. About 40 million tons of banana peels are generally discarded annually and create organic waste problem. Banana peels contain lipids 1.7%, protein 0.9%, crude fiber 31%, carbohydrate 59%, potassium 78.10 mg/g, calcium 19.20 mg/g and iron 0.61 mg/g[20]. This agro-waste has been found an economical adsorbent for adsorption of heavy metals from water.

There are two types of adsorption processes such as physisorption and chemisorption. Physisorption is caused by van der Waals force of interaction between adsorbate molecules and adsorbent. Chemisorption is caused by bounding between adsorbate molecules. Bio-adsorption is physio-chemical interaction between metal and functional group of cell wall.

Bio-adsorption is the mechanism by which inactive date, microbial and biomass is used to bind heavy metals from very dilute aqueous solution. It involves solid phase adsorbent and liquid phase adsorbate. It involves passive uptake of metal immediately and active uptake slowly. Toxic heavy metals do not affect the adsorbent in bio-adsorption. In this method, metal ions stick on to the surface of biological components. It requires the biological materials which have high metal binding capabilities and specific heavy metal selectivity. It may involve one process or a blend of processes like adsorption, electrostatic interaction, chelation, micro-precipitation and ion exchange[21]. These methods are economical, renewable and

locally available adsorbents methods for water treatment such as orange peel, banana peels, rice husk, waste tea, sugarcane bagasse, coconut husk, etc. The adsorption capacity of divalent heavy metal ions (Cu^{2+}, Zn^{2+}, Co^{2+}, Ni^{2+} and Pb^{2+}) onto acid (HNO_3) and alkali (NaOH) treated banana peels has been studied. The adsorption capacity was found to be in the order of $Pb^{2+} > Ni^{2+} > Zn^{2+} > Cu^{2+} > Co^{2+}$. The maximum metal adsorptions were recorded as 7.97, 6.88, 5.80, 4.75, and 2.55 mg/g for Pb^{2+}, Ni^{2+}, Zn^{2+}, Cu^{2+} and Co^{2+}, respectively[22]. The practical applicability of banana peel has been assessed to remove arsenic from contaminated water samples collected from 8 different areas of Sindh, Pakistan. The equilibrium adsorption experiments were performed out at 25 °C in the range of 0.5-1000 mg/L of arsenic using 100 mg of an adsorbent obtained from banana peel. Adsorption of both species was found to be independent of pH and 75% and 95% adsorption was recorded for As (III) and As (V), respectively[23]. The potential of application of banana peel (BP) as a bio-adsorbent for adsorption of As (III) ion from contaminated water was evaluated. Equilibrium isotherms and kinetics were obtained and the effects of solution pH, temperature, dosage and contact time were studied in batch experiments. The maximum percentage removal (82.23%) of As(III) ion was obtained at optimized pH 7, contact time (tc) of 90 min, dosage (dc) of 8 g, temperature (tc) of 35 °C and 10 mg/L As (III) ion concentration (Ci), respectively. Equilibrium was well described by Freundlich isotherm model correlation coefficient value (R2= 0.993). Moreover, it was also found that adsorption kinetics favored pseudo-second order model with high correlation coefficient value (R2= 0.998)[24]. This paper deals with preparation of activated carbons from banana peel, their characterizations and application to the removal of As(III) ions present in water system.

Materials and methods
Materials
Banana Peels were used as precursor material for the preparation of adsorbent. Ripe banana peels (Dwarf Cavendish variety) used for the study were collected from

local market in Nayabazar, Kirtipur Kathmandu. These were cleaned with distilled water to remove sand and other debris. Cleaned peels were dried in sunlight to remove moisture. The dried banana peels were cut into small pieces and was ground into fine powder using grinder. It was sieved to particle size ≤90 μm and was stored in air tight plastic container to obtain raw banana peel powder.

Preparation of activated carbon

Banana peels powders were subjected to pyrolysis in different environments in the tube furnace (21100 Tube Furnace, USA). It was heated to 700 ℃ for 1 hour in open air, nitrogen gas and the mixture of nitrogen gas and water steam at 60-80 ℃. The heating rate was fixed at 10 ℃/min and flow rate of nitrogen gas was 100 mL/min. Thus, three different types of activated carbons, activated carbon prepared in open air (O_2-BP), activated carbon prepared in nitrogen gas (N_2-BP), activated carbon prepared in nitrogen gas and water steam (N_2+H_2O-BP).

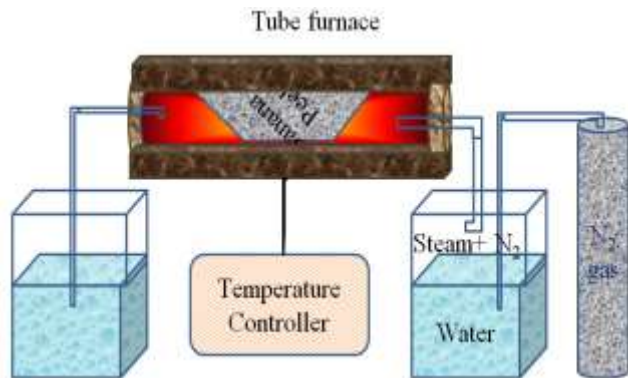The schematic diagram of the pyrolysis of banana peels is shown in Figure 1.

Figure 1: Schematic diagram of the pyrolysis of banana peels

The technique is environment friendly since the gas is passed from one side of the tube and other side contains the outlet of black smoke dipped into water trough. The tube, containing banana pieces, was placed inside the furnace heated accordance to the need using temperature controller. Atmosphere inside the tube was changed as per the requirements. This was done either by passing air (oxygen gas) or nitrogen gas or the mixture of nitrogen gas and water steam.

Preparation of stock and standard solutions

Stock solution of As (III) 1000 ppm from arsenic trioxide (As_2O_3, LR Grade Loba Chemie, dried at 110 ℃ for an hour) was prepared. The standard arsenic solutions of required concentration were prepared by appropriate dilution of stock arsenic solution by adding 1 mL HCI in volumetric flask.

Ammonium molyddate reagent (I) 500 mL was prepared from ammonium heptamolybdate [$(NH_4)_6M_{O7}O_{24}.4H_2O$, LR Grade Qualigens 87.5 mL], 140 mL of Conc. sulphuric acid in distilled water cautiously

Ammonium molybdate reagent (II) was prepared from ammonium molybdate (20.05 g). Ammonium molybdate reagent (I) (198 mL) was added to the reagent (II), cooled and diluted up to 500 mL with distilled water. The concentration of the reagent (II) was 5%. The 0.5 M ammonium molybdate working solution was prepared from dilution method. The potassium permanganate ($KMnO_4$, LR Grade, Qualigens) solution of 0.1 N was prepared. The 1.5 N sulphuric acid 250 mL was prepared in distilled water. The 0.5 M hydrazine hydrate solution was prepared by taking 2.44 mL and diluted to 100 mL. Buffer solutions of pH 4.01, 7 and 9, were employed for calibration of pH meter.

Adsorption Studies

Preparation of calibration curve for methylene blue solution

For preparation of calibration curve, at first the maximum absorbance was designed. Here it was done by preparing 5 mg/L solution of methylene blue. The absorbance was measured against wavelength ranging from 600 to 690 nm using spectrophotometer (Aquarius, CE 7200, England). The maximum absorbance (λ_{max}) obtained was at 660 nm. After that the methylene blue solution of 1, 2, 3, 4, 5, 6, 7, 8, 9 and 10 mg/L were prepared in 25 mL volumetric flasks. The absorbance of all these solutions was taken at 665 nm wavelength. A plot of absorbance versus concentration thus gives a calibration curve for methylene blue solution.

Specific surface area determination

To determine the specific surface area of the raw and activated carbons, the Langmuir adsorption isotherm model was used. For this, 25 mg of raw and activated carbon was weighed out accurately and transferred to 25 mL conical flask containing varying concentration of methylene blue (MB) solutions (20-100 mg/L).

The solutions were then shaken for 4 continuous hours in an orbital shaker (SSL$_1$ Shaker, Stuart, UK). It was then allowed to rest for half an hour doing so the carbon settled down and the supernatant solution was pipetted out. The absorbance of the resultant solutions was taken at 665 nm wavelength. From the Langmuir adsorption isotherm, Q$_m$ value was calculated and using the formula of specific surface area equation (1)[25], the specific surface area of the activated carbon was determined.

$$S_{MB} = \frac{N_g \times a_{MB} \times N \times 10^{-20}}{M} \quad \ldots\ldots\ldots \quad (1)$$

Where, S$_{MB}$ is the specific surface area in 10^{-3} km^2 kg^{-1}. The Q$_m$ is the amount of adsorbate per unit gram of adsorbent required to form a monolayer coverage, a$_{MB}$ is occupied surface area of one molecule of MB = 197.2A^2, N is Avogadro's number (6.023×10^{23}), M is the molecular weight of MB (319.85 g/mol).

Preparation of calibration curve of As (III) ion

Arsenic solution containing 0.1, 0.2, 0.3, 0.4, 0.5, 0.6, 0.7, 0.8, 0.9 mg/L and blank solution were prepared in 25 mL volumetric flask by following methods:

The required amounts of diluted solutions were pipetted out and transferred into 25 mL volumetric flasks to each solution 4.5 mL of 1.5 N sulphuric acid was added then one drop of 0.1 N potassium permanganate was added, stirred for one minute. Three mL of 0.5% ammonium molybdate and 3 mL of 0.5 M hydrazine hydrate were added. The volume was made up to mark by adding distilled water. For full color development the above solutions were left for 20 minutes at room temperature. The absorbance of each solution was measured at 840 nm against blank solution with the help of spectrophotometer. A plot of absorbance versus concentration of arsenic was made.

Effect of pH

The pH is an important parameter influencing the adsorption behavior of adsorbate onto bioadsorbent surface due to its impact on both the surface binding-sites of the bioadsorbent and the metal ion solution. For the pH studies of As(III) adsorption, the initial concentration and volume of solutions taken were 20 mg/L and 25 mL respectively. The solutions were taken in 100 mL Erlenmeyer flask and the pH of the solutions was adjusted from 4 to 10 using appropriate strength of NaOH and HNO$_3$ solutions by the help of pH meter (Model 270, Denver Instrument, Japan). To each flask, 25 mg N$_2$+H$_2$O-BP adsorbent was added and then shaken in mechanical shaker for 24 hours at speed of 200 rpm. After shaking, each solution was filtered immediately using Whatman 41 filter paper and the equilibrium pH of the filtrate was noted. The filtrates were analyzed to determine the equilibrium concentration of arsenic. With the help of initial and equilibrium concentrations, the percentage adsorption of arsenic at each pH was determined. Thus, the optimum pH for the adsorption of arsenic was evaluated.

Adsorption Isotherm Studies

The effect of arsenic concentrations on the adsorption was studied under optimum pH. The adsorption isotherm study was done with different initial concentration of As (III) ion ranging from 20 to 500 ppm with 25 mg of N$_2$+H$_2$O-BP adsorbent. The solutions were shaken in a mechanical shaker for 24 hours at speed of 200 rpm. The equilibrium concentrations of arsenic after adsorption were determined by Molybdenum Blue method using spectrophotometer. Two adsorption isotherm models Langmuir model and Freundlich model had been tested to study the adsorption isotherm study.

Kinetic studies

The adsorption kinetic experiments were performed at corresponding optimum pH for AS(III) ion by equilibrating.

For the study of kinetic behavior, 25 mL of 20 ppm arsenic solutions in 100 mL Erlenmeyer flask containing 25 mg N_2+H_2O-BP adsorbent was used. These flasks were shaken for different length of time, at speed of 200 rpm. The kinetics were investigated by taking out flasks at desired period of contact time and immediately filtered through Whattman 41 filter paper to obtain filtrates and the concentrations in the filtrates were determined spectrophotometrically. The data obtained was tested with pseudo-first order, pseudo- second order and intra-particle diffusion models.

X-ray diffraction (XRD) measurement

All the three samples prepared in different environments and raw BP, without any adsorption, were analyzed for the phase detection using X-ray Diffractometer with monochromatic Cu Kα radiation (D2 Phaser Diffractometer, Bruker, Germany) at Nepal Academy of Science and Technology (NAST). The samples were scanned at 2θ angle from 10 to 80º.

Fourier Transform Infrared (FTIR) analysis

All the three samples prepared in different environments and raw BP, without any adsorption were analyzed using FTIR Spectrophotometer (IR Tracer- 100 SHIMADZU, Japan) at Nepal Academy of Science and Technology (NAST) from frequency 400 to 4000 cm^{-1}.

Results and discussion

Characterization of adsorbent materials
X-ray diffraction (XRD) analysis

The XRD patterns of raw and activated banana peels formed by physical activation are shown in Figure 2. The XRD profiles for pyrolytic banana peels exhibited sharp peaks which indicate changes in the structure of activated carbon. It was confirmed that the pyrolysis temperature at 700 ºC of activated banana peel carbon were thermally decomposed to crystalline graphitic allotropic form of carbon at 28.6 and 31.7º, chaoite peaks at (24.5º and 30º). The peaks appeared at 66.60º was characterized as alumina and that at 73.9º as silicon dioxide.
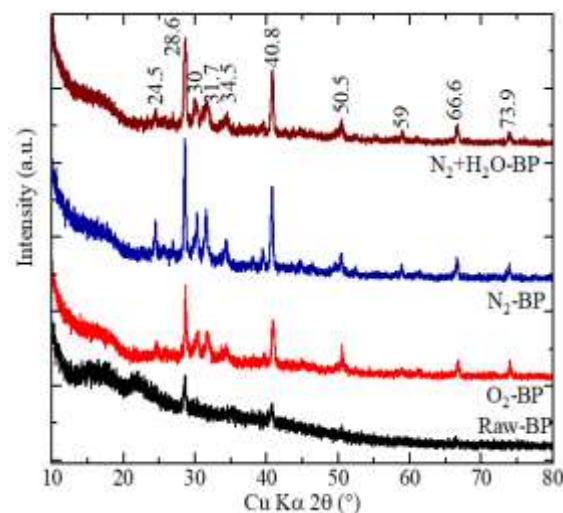

Figure 2: XRD patterns of Banana peel and its activated carbon formed in various environments

The XRD patterns implied pyrolytic products were not pure and have some impurity. Impurities include some amorphous carbon (i.e. activated carbon) at 59º, Fe_3C at 40.8º, Fe_2O_3 at 34.5º and K_2O at 50.5º. It suggests that pyrolysis reaction was not complete and amorphous carbon was remained. For, Fe_3C and Fe_2O_3, it was suspected that Fe metal dissociated from banana peels and reacted with carbon and oxygen. In the case of K_2O, as banana peels had high content of potassium, it reacted with oxygen during oxidation reaction[26].

From Figure 2, the peak for activated carbon is intense for physically activated banana peels than raw banana peels which contribute to high adsorption capacity. The high intensity XRD peaks of physically activated carbon is due to the increase in the porous structure of banana peels after activation compared to raw banana peels.

Fourier Transform Infrared spectra analysis

The FTIR spectra of raw banana peel (BP) together with its activated samples are shown in Figure 3.
The FTIR spectra of BP were obtained to understand nature of functional groups in Banana peels. The FTIR displayed a number of peaks indicating complex nature of adsorbent. The spectrum of (BPAC) has a broad absorption peaks at around 3400–3500 cm^{-1}, indicates the presence of carboxylic acid and amino groups. The absorption band at

2900-2970 cm^{-1} could be assigned to asymmetric vibration of –CH. The stretching vibration bands 1600-1650 cm^{-1} is due to asymmetric stretching of the carboxylic C=O double bond. A band at 1365-1400 cm^{-1} is of phenolic –OH and –C=O stretching of carboxylates. Peaks in the region of 832 cm^{-1} appeared as a broad peak can be attributed to N containing bioligands[27]. The peaks at 1054.40–534.42 cm^{-1} were attributed to Si-O stretching and Si-O bending indicating of the silica presence[24].
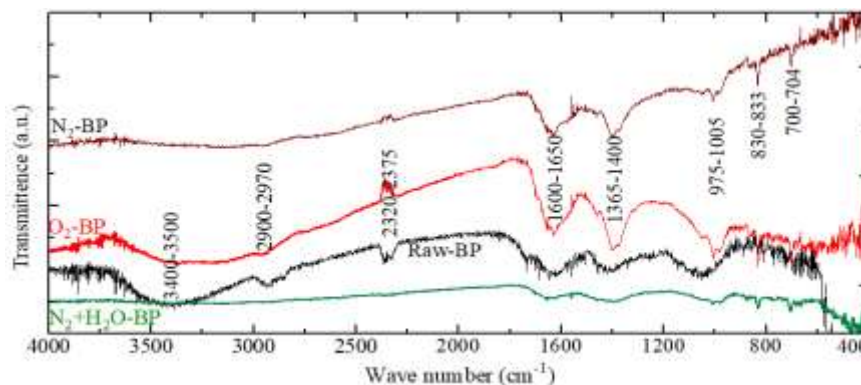

Figure 3: FTIR spectra of banana peel and its activated carbon formed in various environments

The difference between FTIR spectra of raw and activated banana peels revealed the loss of some functional groups in activated BP due to heat treatment and may be due to the presence of large number of micropores. There is removal of less stable volatile matters in the form of fumes composed of oxygen derivatives during carbonization and activation process increasing the number of pores between the carbon atoms. So, physical activation permits more accurate pore size distribution.

The λ$_{max}$ determination and calibration curve of methylene blue solution

The absorbance of methylene blue with the variation of wavelength confirmed the maximum absorbance at 665 nm which matched with the previous report[28]. The calibration of the methylene blue solution showed the linear relationship between the adsorbance and the concentration up to 10 mg/L and thus follows Beer-Lambert's law. This method is applicable from the range of 0.025-100 ppm. For higher concentrations of the methylene blue solution further dilution required.

Specific surface area determination

The linearized Langmuir plots for the adsorption of methylene blue on raw and activated carbon are shown in Figure 4.

The specific surface areas of raw and activated carbons were calculated with the help of slopes obtained from the curves and tabulated in Table 1.
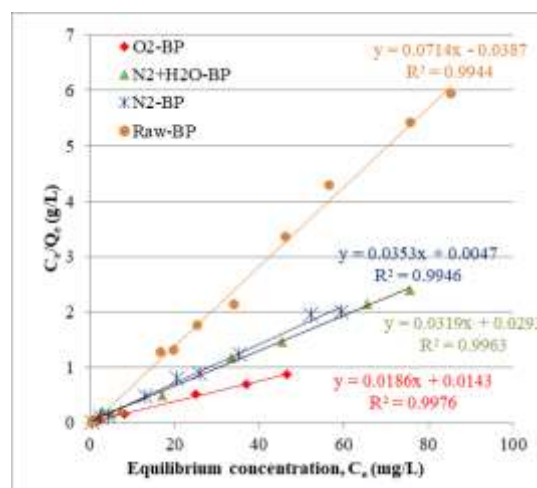

Figure 4: A plot of C_e/Q_e versus C_e of raw and activated carbonS

Table 1. Langmuir parameters for adsorption of methylene blue

Types of BP	Langmuir Parameters			Specific surface area (m²/g)
	Q_m (mg/g)	b (L/mg)	R^2	
Raw BP	14.29	0.99	0.9944	53.04
N_2+H_2O-BP	28.57	8.7	0.9963	106.09
N_2-BP	31.25	1.28	0.9946	116.04
O_2-BP	55.55	1.308	0.9976	204.23

The specific surface area of raw BP was the minimum among these four samples and that of O_2-BP was the maximum. The minimum specific surface area of raw BP is due to plain surface with no pore opening, when raw BP is activated, the surface contains widely scattered pores and carbon percentage increases. During carbonization and activation process in physical activation less stable volatile matters are removed in the form of fumes composed of oxygen derivatives. The O_2-BP has the maximum specific surface area due to high ash content. During N_2+H_2O activation, low ash content is formed on the surface due to removal of ash by the flow of nitrogen gas[29].

Following relation was used for calculating activation burn off of activated banana peels[29]:

$$\text{Activation burn off (\%)} = \frac{\text{Mass loss (g)}}{\text{Original mass of char}} \times 100\% \quad \cdots (2)$$

The yield of activated carbon obtained from banana peel with the help of above equation (1) is tabulated in the following Table 2.

Table 2. Yield of activated carbon (AC) by physical activation [Weight taken was 25.0 g]

Adsorbent	Wt. after activation	Activation burn off (%)	Yield of AC %
N_2+H_2O-BP	06.23	74.668	25.33
N_2-BP	09.74	61.03	38.97
O_2-BP	11.22	55.12	44.88

The highest burn off of char is due to steam activation of banana peels as steam reforming reaction of char forming carbon monoxide and hydrogen in outer as well as in micro pore surface which is faster in present of steam and yield of AC is decreased.

Determination of λ_{max} and calibration of As (III) solution

The variation of absorbance of As (III) solution with wavelength confirmed the maximum absorbance (λ_{max}) of 840 nm. The solution has obeyed Beer-Lambert's law up to the concentration of 1000 ppb. Hence the applicable range of the method is up to 1000 ppb.

Effect of pH

The effect of pH on adsorption process is illustrated in Figure 5 which shows the relationship between adsorption (%) and the initial pH in the adsorption of As(III) ion onto N_2+H_2O-BP at initial concentration of 20 ppm. The pH was varied from 4 to 10. The maximum adsorption was found at pH 7, which was 77.53% which was assigned as optimum pH. At pH lower than 7, H^+ ion concentration is high and As (III) exist as neutral H_3AsO_3, in the pH 0-7.

Therefore, electrostatic repulsion between metal ion and H^+ increased and low removal of As (III) ion was obtained.
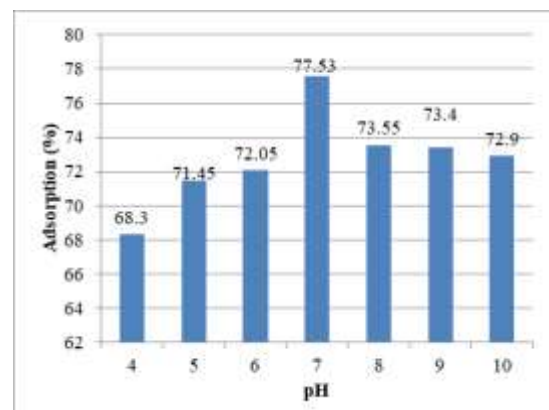

Figure 5: Effect of adsorption as a function of initial pH

When pH increases, there is decrease in positive surface charge because of the deprotonation of adsorbent functional groups which results in lower electrostatic repulsion between the H_3AsO_3 of N_2+H_2O-BP favoring adsorption. The surface of N_2+H_2O-BP becomes negative which increase in pH leading to attractive forces between H_3AsO_3 and N_2+H_2O-BP. The As (III) exists as negatively charged $H_2AsO_3^-$ as in anionic form and its adsorption on the negatively charged surface is unfavorable and the adsorption of As (III) is decreased[24].

Adsorption isotherm of As (III)

Adsorption isotherm is a curve which relates the amount of adsorbate adsorbed per unit mass of adsorbent to the equilibrium concentration at constant temperature. In other words, adsorption isotherm is a graphical representation of

the amount of adsorbate adsorbed per unit mass of the adsorbent as a function of the amount of adsorbate left in bulk solution at equilibrium at constant temperature. Several models have been developed to describe the adsorption phenomenon but the Langmuir and Freundlich adsorption isotherms are the well-known models used to analyze adsorption behavior.

In 1918, Langmuir established the first quantitative model of adsorption. This model has been successfully applied for the adsorption of solute from a liquid solution, which involves active adsorbent sites, homogenous surface for adsorption with the formation of monolayer coverage and adsorption is independent of the occupation of neighboring sites[30]. The Langmuir isotherm is used to estimate the maximum adsorption capacity corresponding to complete monolayer coverage on the adsorbent surface. The linearized form of Langmuir adsorption isotherm is given by the following equation:

$$\frac{C_e}{Q_e} = \frac{1}{Q_m b} + \frac{C_e}{Q_m} \quad \cdots \quad (3)$$

Where Q_e (mg/g) is the amount of adsorbate adsorbed per unit mass of adsorbent at equilibrium, C_e (mg/L) is the equilibrium concentration of the adsorbate, Q_m (mg/g) is the maximum adsorption capacity and 'b' (L/mg) is the Langmuir adsorption equilibrium constant. A plot of C_e/Q_e against C_e gives a straight line with slope $1/Q_m$ and intercepts $1/Q_m b$ from which Q_m and 'b' can be determined. The essential characteristics of Langmuir isotherm can be expressed in terms of dimensionless constant separation factor or equilibrium parameter R_L defined by relation[31],

$$R_L = \frac{1}{(1 + bC_i)} \quad \cdots \quad (4)$$

Where, b = Langmuir constant and C_i = Initial concentration of As (III)

The equilibrium parameter, R_L indicates the shape of isotherm and nature of the adsorption process ($R_L > 1$ unfavorable, $R_L = 1$ linear, $0 < R_L < 1$ favorable, $R_L = 0$ irreversible). The value of R_L between 0 and 1 indicates that

adsorption is favorable. However, the Langmuir model gives no mechanistic aspects of adsorption.

The adsorption data obtained can also be analyzed with Freundlich adsorption model. In 1939 Freundlich established relationship that describes the adsorption phenomenon[32]. The linear from of the Freundich isotherm is given by the equation:

$$\log Q_e = \log K_F + \frac{1}{n} \log C_e \quad \cdots \quad (5)$$

Where Q_e (mg/g) is the amount of adsorbate adsorbed per unit mass of adsorbent, C_e (mg/L) is the equilibrium concentration of the adsorbate, K_F [(mg/g) (L/mg)$^{1/n}$] and n (g/L) are Freundlich equilibrium coefficients, which are considered to be the relative indicators of adsorption capacity and adsorption intensity. The $\log Q_e$ is plotted against $\log C_e$ a straight line is obtained with slope $1/n$ and intercept $\log K_F$. From this plot, the value of $1/n$ and K_F can be determined. The value of $1/n$ between 0 and 1.0 indicates the favorable adsorption of adsorbate.

The adsorption study of As (III) onto $N_2 + H_2O$-BP was done at optimum pH 7 and varying the concentration of As (III) from 20-500 ppm. The slopes and intercepts of the linearized Langmuir and Freundlich plots were used to calculate the Langmuir and Freundlich parameters for the adsorption of arsenic on the adsorbent $N_2 + H_2O$-BP and shown in Table 3.

Table 3. Langmuir and Freundlich parameters and correlation coefficient with experimental Q$_{max}$ for As (III)

Langmuir isotherm				
Q$_{max}$ (mg/g)	b (L/mg)	R^2	ΔG (KJ/Mol)	R$_L$
142.86	0.037	0.9934	-20.04	0.574
Freundlich isotherm				
K$_F$ (L/g)		n		R^2
11.53		2.22		0.8738

The negative value of free energy (ΔG) in adsorption process reveals the spontaneous nature and feasibility of the bio-adsorption process for the adsorption of As (III) on to N_2+H_2O-BP. The value of ΔG confirms the adsorption process is favored by physio-adsorption. The above table shows the value of n is 2.22, which shows good adsorption of As (III) onto activated banana peels. Since, for good adsorption the value of n should lie between 2 to 10[33].

The adsorption of As (III) ion onto N_2+H_2O-BP followed Langmuir model which is supported by its high R^2 (coefficient of determination) value. The Langmuir adsorption is of monolayer adsorption model and removable ions are taken up independently on single type of binding site in such a way that the uptake of first ion does not affect the adsorption of second ion.

The adsorption of As(III) as a function of equilibrium concentration of As(III) is shown in Figure 6 where circular points are experimental data points and solid and dotted line curves are calculated Langmuir and Freundlich curves. The Q_m value obtained from Langmuir was found to be 142.86 mg/g, which is significantly higher than previously reported adsorbents shown in Table 4.

Comparison of the maximum adsorption capacity (Qmax) of the N2+H2O-BP with earlier investigated adsorbents reveals that N2+H2O-BP possesses higher potentiality towards the adsorptive removal of As(III) from aqueous solution.
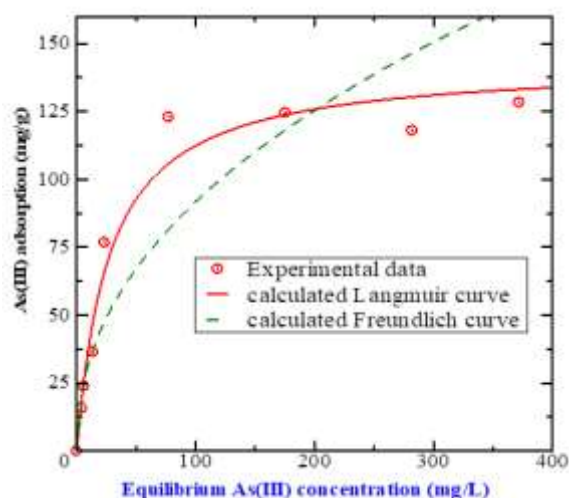

Figure 6: Absorption isotherm for the determination of As(III) onto N_2+H_2O-BP

Table 4. Comparison of maximum adsorption capacity (Q_{max}) of the N_2+H_2O-BP with earlier investigated adsorption.

S. No.	Adsorbent and species	Q_{max} (mg/g)	Source
1	Phosphorylated orange juice residue	68.18	29
2	Activated olive pulp and olive stone	1.39	33
3	Spinacia oleracea (Spinach) Leaves	58.48	28
4	Fe loaded pomegranate waste	50.00	34
5	Zr(V) loaded orange waste gel	130.00	35
6	Thioglycolated sugarcane	0.085	36
7	Steam activated banana peels (i.e. N_2+H_2O-BP)	142.86	Present work

The value of the parameter R_L at different initial concentration of As (III) ion solution from 20 to 500 ppm was calculated with the help of equation (5). It was found that the value of R_L at different initial concentration of As (III) ion lies between 0 and 1 which indicates the favorable adsorption of As (III) on activated banana peels.

Kinetic studies

The kinetic mechanism that controls the biosorption process onto N_2+H_2O-BP was evaluated by using pseudo-first-order, pseudo-second-order and intraparticle diffusion models. The pseudo-first order kinetic model is applicable for the reversible reaction with an equilibrium being established between liquid and solid phase. The differential from of pseudo-fist order rate equation is generally expressed as[37]:

$$\frac{dQ_t}{dt} = K_1(Q_e - Q_t) \quad \cdots \quad (6)$$

Where, Q_e (mg/g) is the amount of adsorbate adsorbed at equilibrium and Q_t (mg/g) is the amount of adsorbate adsorbed at any time 't'. Similarly, K_1 (min^{-1}) is the rate constant of pseudo-first order adsorption.

After integration and applying boundary condition, t = 0 to t and Q_t = 0 to Q_t the linearized from of equation becomes:

$$\log(Q_e - Q_t) = \log Q_e - \frac{K_1}{2.303} t \quad \cdots \quad (7)$$

The plot of log $(Q_e - Q_t)$ versus 't' should give a straight line from which K_1 and Q_e can be determined from slopes and intercepts of the plot respectively.

The pseudo-second order kinetic model is used to study the kinetics of adsorption of adsorbate, which states that the rate of occupation of adsorption sites is proportional to the square of the number if unoccupied sites[38]. It is generally expressed as:

$$\frac{dQ_t}{dt} = K_2(Q_e - Q_t)^2 \quad \cdots \quad (8)$$

Where K_2 (g/mg·min) is the pseudo-second order rate constant and Q_e and Q_t are the amount of adsorbate adsorbed at equilibrium and any time 't' respectively.

After integration and applying boundary conditions, t=0 to t and $Q_t = 0$ to Q_t the equation becomes:

$$\frac{1}{Q_t} = \frac{1}{K_2 Q_e^2} + \frac{1}{Q_e}t \quad \cdots\cdots\cdots \quad (9)$$

If the initial adsorption rate is V_0 (mg/g min), then

$$V_0 = K_2 Q_e^2 \quad \cdots \quad (10)$$

The equation can also be written as:

$$\frac{1}{Q_t} = \frac{1}{V_0} + \frac{1}{Q_e}t \quad \cdots \quad (11)$$

Experimentally, the values of Q_e and k_2 can be determined from the linear plot of t/Q_t versus 't' with the slope and intercept of the plot respectively.

In order to identify the diffusion mechanism, the intraparticle diffusion model can be represented as[39]:

$$Q_t = K_i t^{1/2} \quad \cdots \quad (12)$$

Where, k_i is the intraparticle diffusion rate constant and Q_t is the amount of metal ion adsorbed (mg/ g) at time t (min). According to this model, the plot of q versus $t^{1/2}$ yields a straight line passing through the origin if the adsorption process obeys the sole intraparticle diffusion model.

With the help of the slopes and intercepts of the plots obtained from the equations (7) and (9), kinetic parameters of pseudo first and pseudo second order rate expressions of the adsorption of As(III) onto N_2+H_2O-BP were calculated and are tabulated in the following Table 5:

Table 5. Kinetic Parameters of As(III) adsorption onto N_2+H_2O-BP

Pseudo First Order Model			Pseudo Second Order Model		
Q_e (mg/g)	K_1 (min⁻¹)	R^2	Q_e (mg/g)	K_2 (g/mg min)	R^2
4.71	0.0138	0.8716	18.52	0.0111	0.9963

The results presented in Table 5 demonstrated that the coefficient of determination values (R^2) for the pseudo-first and pseudo-second order kinetic models are 0.8716 and 0.9963 respectively indicating that the bioadsorption of As(III) onto steam activated banana peels (N_2+H_2O-BP) follows pseudo-second order model with the rate constant value 0.0111 g/(mg·min). The plot of Q_t and $\sqrt{t}$ in Figure 7, does not pass through the origin which indicates that the intra-particle diffusion is not the rate limiting step. It could be stated that this process is complex and may involve more than one mechanism.
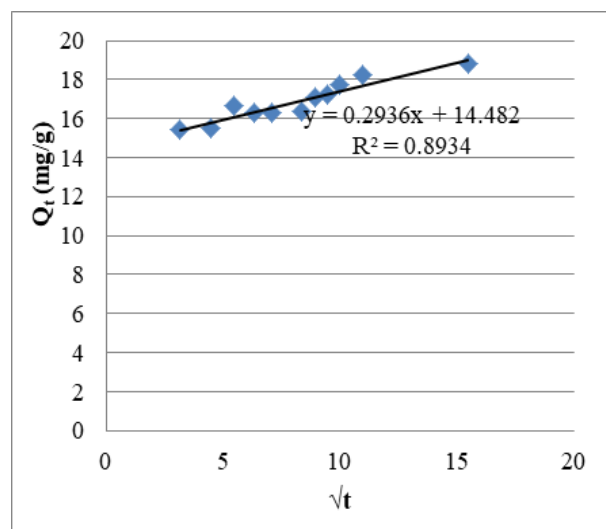

Figure 7: Plot of Q_t verses $\sqrt{t}$ plot for the adsorption of As (III) on steam activated banana peels (N_2+H_2O-BP)

The kinetic plot of the adsorption of As(III) as a function of reaction time is shown in Figure 8 where traingle points are experimental data points and solid line curve is calculated pseudo 2nd order curve. From the Figure 8, it is clear that the maximum adsorption occurred within 10 minutes. It was found that the adsorption rate was rapid at first and then attains equilibrium with further reaction time.
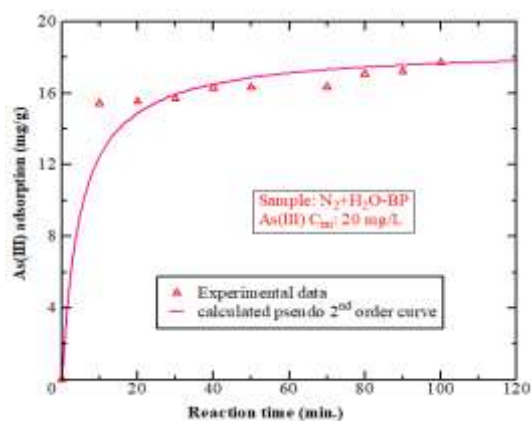
Figure 8: Effect of contact time for the adsorption of As (III) on steam activated banana peels (N₂+H₂O-BP)

After reaching the saturation points there was no significant change in the rate. The initial rapid increase in the rate was due to the availability of more active sites. As the time passed the number of active sites became less and finally the equilibrium state was achieved.

Conclusion

Various activated carbons were prepared from banana peels and were characterized by XRD, FTIR and methylene blue adsorption methods. The specific surface area of raw BP, O_2-BP, N_2+H_2O-BP, N_2-BP were 53.04, 204.23, 106.09, 116.04 m^2/g respectively. The XRD peaks indicated the presence of crystalline graphitic allotropic form of carbon, chaoite, alumina, silicon trioxide, activated carbon, Fe_3C, Fe_2O_3 and K_2O. The FTIR spectra of raw and activated banana peels revealed the loss of functional groups due to heat treatment. The optimum pH was 7 for As (III) adsorption. The adsorption isotherm study showed that the Langmuir model fitted better. The maximum adsorption capacity was 142.86 mg/g. The experimental data fitted well to pseudo-second order kinetic model with rate constant value 0.0111 g/(mg·min). The value of ΔG obtained from Langmuir equation was -20.04 KJ/Mol., which indicated the spontaneous adsorption. The value of separation parameter R_L revealed good adsorption of As (III) onto banana peels.

References

1. Lakshmipathy, R., Sarada, N. C. and Jayaprakash, N. 2015. Agricultural wastes as low cost adsorbents for sequestration of heavy metal ions and synthetic dyes from aqueous solution: A mini review. *International Journal of Chem. Tech. Research.* **8(5)**: 25-31.

2. Akil, A., Mouflih, M. and Sebti, S. 2004. Removal of heavy metal ions from water by using calcined phosphate as a new adsorbent. *Journal of Hazardous Materials.* **112(3)**: 183-190.

3. Van Halem, D. et al. 2009. Arsenic in drinking water: a worldwide water quality concern for water supply companies. *Drinking Water Engineering and Science.* **2**: 29-34.

4. Thakur, L. S. and Senil, P. 2013. Removal of arsenic in aqueous solution by low cost adsorbent: A short review. *International Journal of ChemTech Research.* **5(3)**: 1299-1308.

5. Sharma, V. and Sohn, M. 2009. Aquatic arsenic: Toxicity, speciation, transformations, and remediation. *Environment International.* **35**: 743–759.

6. Jack, C. N. 2005. Environmental contamination of Arsenic and its toxicological impact on humans. *Environmental Chemistry.* **2(3)**: 146-160.

7. Pous, N., et al. 2015. Anaerobic arsenite oxidation with an electrode serving as the sole electron acceptor: A novel approach to the bioremediation of arsenic-polluted groundwater. *Journal of Hazardous Materials.* **283**: 617–622.

8. Singh, R., et al. 2015. Arsenic contamination, consequences and remediation techniques: a review. *Ecotoxicology and Environmental Safety.* **12**: 247–270.

9. Bodek, I., et al. 1988. Environmental inorganic chemistry: properties, processes and estimation methods. Pergamon Press. USA.

10. Thomas, D., Waters, S. and Styblo, M. 2004. Elucidating the pathway for arsenic methylation. *Toxicology and Applied Pharmacology.* **198(3)**: 319–326.

11. Rossman, T., Uddin, A. N. and Burns, F. J. 2004. Evidence that arsenite acts as a cocarcinogen in skin cancer. *Toxicology and Applied Pharmacology.* **198(3)**: 394–404.

12. Murcott, S. 2012. Arsenic contamination in the world: an international sourcebook. IWA publishing. London. UK.

13. Chatterjee, D., et al. 1995. Arsenic in groundwater in six districts of west Bengal, India: the biggest arsenic calamity in the world. Part 1, *Analyst.* **120**: 643–656.

14. Garelick, H., et al. 2008. *Arsenic pollution sources, Reviews of Environmental Contamination and Toxicology.* **197**: 17-60.

15. Panthi, S. R., Sharma, S. and Mishra, A. K. 2006. Recent status of arsenic contamination in groundwater of Nepal- A review. *Kathmandu University Journal of Science, Engineering and Technology.* **2(1)**: 1-11.

16. Maharjan, M., et al. 2006. Prevalence of arsenicosis in terai, Nepal. *Journal of Health, Population and Nutrition.* **24(2)**: 246-52.

17. Mondal, P., Balomajumder, C. and Mohanty, B. 2006. Laboratory based approaches for arsenic remediation from contaminated water: recent developments. *Journal of Hazardous Materials.* **137(1)**: 464-479

18. http://www.asiafarming.com/fruit farming (cited in Oct. 2, 2015).

19. http://www.icimod.org (cited in July 23, 2015).

20. Anhwange, B. A., Ugye, T. J. and Nyiaatagher, T.,D. 2009. Chemical composition of Musa sapientum (banana) peels. *Electronic Journal of Environmental, Agricultural and Food Chemistry*. **8(6)**: 437-442.

21. Monisha, J., et al. 2014. Biosorption of few heavy metal ions using agricultural wastes. *Journal of Environment Pollution and Human Health*. **2(1)**:1-6.

22. Annadurai, G., Juangand, R. S. and Lee, D. J. 2002. Adsorption of heavy metals from water using banana and orange peels. *Water Science and Technology*. **47(1)**: 185–190.

23. Memon, S. Q., Bhander, M. I. and. Memon, J. R. 2008. Evaluation of banana peel for treatment of arsenic contaminated water. Proceedings of the 1st technical meeting of muslim water researchers co-operation (MUWAREC) Malaysia. 104 -107.

24. Kamsonlian, S., Balomajumder, C. and Chand, S. 2012. A potential of biosorbent derived from banana peel for removal of As (III) from contaminated water. *International Journal of Chemical Sciences and Applications*. **3**: 269-275.

25. Itodo, A. U., Itodo, H. U. and M. K. Gafar. 2010. Estimation of specific surface area using Langmuir isotherm method. *Journal of Applied Sciences and Environmental Management*. **14(4)**: 141-145.

26. Mopoung, S. 2011. Occurrence of carbon nanotube from banana peel activated carbon mixed with mineral oil. *International Journal of the Physical Sciences*. **6(7)**: 1789-1792.

27. Mahmoud, M. S. 2014. Banana peels as an eco-sorbent for manganese ions. *International Journal of Agricultural and Biosystems Engineering*. **8(11)**: 1201-1207.

28. Jha, P. K. and Jha, V. K. 2021. Arsenic adsorption characteristics of Adsorbent prepared from spinacia Oleracea (spinach) leaves. *Scientific World*. **14**: 51-61.

29. Ghimire, K. N., et al. 2003. Adsorptive separation of arsenate and arsenite anions from aqueous medium by using orange waste. *Water Research*. **37(20)**: 4945-4953.

30. Langmuir, I. J. 1918. The adsorption of gases on plane surfaces of glass, mica and platinum, *Journal of the American Chemical Society*. **40**: 1361-1403.

31. Maron, S. H. and Pruton, C. F. 2001. *Principles of Physical Chemistry* (4th edition). Macmillan Company. New York.

32. Freundlich, H. and Heller, W. 1939. The Adsorption of cis- and trans-Azobenzene. *Journal of American Chemical Society*. **61**: 2228-2230.

33. Budinova, T., et al. 2006. Removal of Arsenic (III) from aqueous solution by activated carbons prepared from solvent extracted olive pulp and olive stones. *Industrial & Engineering Chemistry Research*. **45**: 1896-1901.

34. Thapa, S. and Pokhrel, M. R. 2012. Removal of As (III) from aqueous solution using Fe (III) loaded pomegranate waste. *Journal of Nepal Chemical Society*. **30**: 29-36.

35. Biswas, B. K., et al. 2008. Adsorptive removal of As (V) and As (III) from water by a Zr (IV)-loaded orange waste gel. *Journal of Hazardous Materials*. **154**: 1066-1074.

36. Roy, P., et al. 2013. Removal of arsenic (III) and arsenic (V) on chemically modified low-cost adsorbent: batch and column operations. *Applied Water Science*. **3**: 293-309.

37. Lagergren, S. 1898. Zur theorie der sogenannten adsorption geloster stoffe. *Kungliga svenska vetenskapsakademiens. Handlingar*. **24**:1-39.

38. Ho, Y. S. and McKay, G. 1999. Pseudo-second order model for sorption processes. *Process Biochemistry*. **34(5)**: 451-465.

39. Karmacharya, M. S. 2017. Physicochemical characteristics of activated carbon obtained from waste tire and its alumina composite. PhD Thesis, Tribhuvan University, Kathmandu, Nepal.

■